Journal of Modern Technology
Vol. 02, No. 01, May 2025, pp. 264-282.
DOI: https://doi.org/10.71426/jmt.v2.i1.pp264-282 , E-ISSN: 3049-3102
Homepage: https://review.journal-of-modern-technology.com/index.php/jmt/index

A Systematic Approach for Protective Relay Coordination and Transient Stability Examination in Energy Networks with Substantial DG Penetration

Milad Taheri [1], Mohammad Parhamfar [2*], Alireza Hajarkesht [3], Alireza Soleimani [4], Aykut Fatih Güven [5], Anna PINNARELLI [6]

[1] PhD Scholar, Department of Electrical Engineering, Islamic Azad University of Najaf Abad, Isfahan, Iran.
Email: milad.taheri@iau.ir, ORCID: https://orcid.org/0009-0001-0619-6601
[2*] Independence researcher and Complex issues analyst, Isfahan, Iran. Email: drparhamfar@gmail.com, ORCID: https://orcid.org/0000-0002-3442-8270
[3] M.S. Degree in the Department of Electrical Engineering, Shahrood University, Karaj, Iran. Email: Ali.Hkasht@shahroodut.ac.ir
[4] Department of Mechanical, Energy and Management Engineering – DIMEG, University of Calabria, Rende 87036, Italy.
Email: alireza.soleimani@unical.it , ORCID: https://orcid.org/0000-0002-9081-6630
[5] Department of Electrical and Electronics Engineering, Engineering Faculty, Yalova University, 77200 Yalova,Türkiye.
Email: afatih.guven@yalova.edu.tr , ORCID: https://orcid.org/0000-0002-1071-9700
[6] Department of Mechanical, Energy and Management Engineering – DIMEG, University of Calabria, Rende 87036, Italy.
Email: anna.pinnarelli@unical.it , ORCID: https://orcid.org/0000-0001-6720-9894

Article Info

Article history:

Received: March 25, 2025
Revised: April 28, 2025
Accepted: May 02, 2025
First Online: May 05, 2025

Keywords:

Distributed generation
Transient stability
Overcurrent relay coordination
Fault location examination
IEEE 33 bus System
Reliability

ABSTRACT

A transient stability examination is crucial in pinpointing the constraints of the electric power systems. On the other hand, the infiltration level of distribution generation influences the constraints in creating safeguards in the power system. Therefore, these two parameters should be regarded as key elements in the power system conservation of the grid. In this work, a transient stability examination of a power system, including DGs, is accomplished to evaluate the protective settings of overcurrent relays (OCRs). For this purpose, the transient stability of DGs is scrutinized under fault conditions at the sites, as well as different DG infiltration degrees. Then, the limitations of DGs in the protective harmonization of OCRs are considered. A novel systematic approach for calculating the modified time multiplier setting (TMS) of OCRs is recommended. The recommended approach maintains coordination among OCRs, and the instability of DG sources is also prevented. Modeling of the IEEE 33 bus system using the ETAP application is used to test the suggested protection scheme's efficacy.

Corresponding Author:

Email address of corresponding author: drparhamfar@gmail.com (Mohammad Parhamfar)

1. INTRODUCTION

Distribution generation mentions producers that are connected to the power distribution system. These assets are placed close to the burden, and if the optimal scale and installation place are picked, they have the potential to

diminish or defer the requirement for capital allocation to the transmission line and distribution framework [1]. Requesting through improved vitality productivity is a fundamental criterion in flexible engineering and sustainable municipal vitality infrastructure for continuous municipal expansion. One of the impactful and streamlined tools for heightening vitality and productivity is the implementation of unified warmth and strength CHP established on DG innovations [2]. Other DG origins are also joined to the strength system and employed depending on geographical situations and other factors. Moreover, vitality productivity enhancements may be hampered by high initial outlays and technological restrictions in adapting to diverse vitality demands across areas. Protective relays are critical assets during fault occurrences in the strength systems. However, if these protective equipment duties are not properly set and are not extensively and thoroughly appraised utilizing strength system examination tools, they may malfunction after a short-circuit fault event and threaten the dependability of the strength system. Strength system examination implemented without adequate emulation of the protective scheme behavior and the dynamic attributes of the system may lead to incorrect assessment of the system's conduct under potential situations.

A vital modeling tool for proper system emulation is a transient stability examination in the positive-sequence time field [3]. The behavior of strength systems in emergencies is primarily influenced by the dynamics of generators and the actions of the shielding system. Next, a major event, the behavior of the strength system is strongly reliant on the protective programs and the system's dynamics, which are managed by the variables of generators, burdens, and control equipment [4]. Protecting distribution frameworks is among the most significant aspects of strength systems. OCRs are a type of protective relay that is commonly utilized in these frameworks. There are a couple of kinds of configurations for these relays: current configurations and time configurations. Proper relay configurations play a significant part in cutting breakdowns caused by faults in strength systems [5]. Additionally, fuses and reclosers are widely utilized protective equipment for distribution system protection, and proper coordination among their duties is essential during fault occurrences. Many studies have handled this issue, offering various resolutions for accomplishing this coordination [6]. In this category, procedures for calibrating the time-current voltage attributes of voltage-based protective equipment (non-standard characteristic curves) are enforced. To implement these procedures, digital protection Equipment based on microprocessors is required. In these references, the required voltage at the start of the line can be easily logged utilizing a voltage transformer at the upstream distribution station. Since this voltage is gauged locally, there is no need for telecommunications infrastructure. The rotor angle stability examination of generators after a fault is a crucial aspect of the strength system's stability. Interferences and sudden modifications, such as short circuits, cause significant modifications in transmission line strength flow, strength angles, and the rotational velocity of synchronous generators. If these interferences are not resolved quickly, the grid will fail to continue operating, thus forfeiting its stability [7]. Many studies have proposed procedures to ensure the steadiness of DG origins in strength systems, particularly in the distribution division. The goal of these procedures is to provide new protective configurations to ensure the simultaneous coordination of protection and the transient stability of DG resources [8].

Reference [8] proposed a new method to safeguard generators from transient instability, utilizing active output strength from the DG generators during faults and CCT to extract the relay attributes. Optimal protection coordination to maintain the transient stability of synchronous generators through communication among relays is proposed in [9]. Soleymani Aghdam et al. [10] recommended utilizing OCRs with two attributes, as standard OCRs cannot meet protection restrictions and transient stability requirements independently. As the fault current increases, the secondary characteristic replaces the primary relay characteristic. Nayanatara et al. [11] introduced a novel procedure for adjusting OCR and ground fault relays in distribution stations of distribution systems, including new renewable production and local grids, utilizing modern numerical relay attributes. This procedure works correctly when there are significant modifications in the fault current based on the layout and configuration of the network. One challenge is verifying the correct coordination and performance of protection systems, especially when merging new renewable production and local grids, as their variable nature can lead to instability during fault situations. Another challenge is the difficulty in achieving optimal protection configurations for overcurrent and earth fault relays, particularly when fault currents fluctuate significantly due to modifications in network layout and configuration, requiring advanced relay attributes for reliable operation. In [12], the authors cited that the integration of DG into distribution systems can disturb protection systems during faults, as inverter-based production restrictions limit fault current to 1–4 Pu, while synchronous or induction generator-based systems inject significantly higher fault currents of 5–10 Pu. Ref. [13] demonstrated that the proposed integrated control and protection strategy, integrating ACLC and single-terminal defect identification, effectively lessens the fault current rise rate by 38.4% and ensures fast error isolation in AC/DC distribution systems under various fault scenarios. However, reference [14] found that the HGS algorithm outperforms GWO and CS in achieving minimum operating times and optimal alignment of DOCRs in strength utility grids with V2G integration, enhancing dependability and productivity. Ref. [15] indicated

that the MHGS procedure successfully decreases relay operation duration and optimally coordinates DOCRs, exceeding traditional HGS and other techniques, while computing for all N-1 unforeseen circumstances in local MGs. Reference [16] focuses on optimizing the configurations of directional OCRs to maintain the stability of distribution systems with local grids. It presents a procedure for appraising the obstacles associated with linking distributed production origins in the distribution system, including network dependability, network stability, and harmonic minimization in the distribution system [17]. The authors in this paper [18] examine the penetration of DGs in distribution networks and their impact on OCRs. The purpose of the paper [19] is to propose a protection scheme with low-bandwidth communication in the time domain for standalone MGs. The utilization of the GA also provides the optimal settings for DOCR, which include relay coordination and the stability of MGs [20]. In reference [21], the authors proposed that the adaptive protection method based on inverse time characteristics can also be utilized for fault location analysis under critical conditions. However, in reference [22], the techniques of TW and DWT were also employed to attempt fault location detection. In reference [23], the authors demonstrated that by utilizing four optimization algorithms, PSO, GA, TLBO, and SFLA, efforts were made to find reduced coordination times. In study [24], it was demonstrated that PSO and GA can also be utilized for optimal coordination to improve the operation of OCRs and reduce their operating time. However, in reference [25], it was presented that for rapid fault detection and isolation, a MAS method is also utilized for control and protection. Pradhan and Jena [26] utilize the dynamic method of negative sequence impedance angle for detecting asymmetrical and high-resistance faults in various locations of the MG. The settings of DOCRs are determined using the AFDBA, creating optimal settings [27]. The results of this research can be used for buildings and related areas [37,38]. Also, this study is important for the move to carbon-zero goals [39,40,41]. The results of the paper can be important for software development teams [42]-[44].

In this research, the primary objective is to address two significant challenges that cause instability in the distribution network and synchronous generators. These challenges are the connection of synchronous generators to the distribution network, which leads to the injection of fault current into the distribution network, and the occurrence of transient 3-phase faults. To address these challenges, a protective algorithm is proposed to establish coordination among OCRs. This algorithm mitigates the instabilities by adjusting the TMS of the OCRs. The proposed protective algorithm is modeled on an IEEE 33 bus distribution system using the ETAP software and is evaluated through five comparative scenarios. The protective algorithm, obstacles, troubles, and previous work are handled in the introduction section. The second section investigates the case study of the IEEE 33 bus system. The third section evaluates the proposed technique for synchronizing CTI and CCT. The fourth section discusses the results and scenarios. The sixth section provides conclusions and suggestions for future work. The advantages of this research are as follows:

- Enhancing the speed, sensitivity, and reliability of OCRs against 3-phase faults in various scenarios.
- Managing fault current injection resulting from the integration of synchronous generator-based DG into the distribution network and mitigating injected fault currents through the coordinated operation of OCRs within the network.
- Improving the coordination time of OCRs and the critical fault-clearing time for 3-phase fault currents in distribution networks with synchronous generator-based DG.
- Enhancing the transient stability of synchronous generators against short circuits, voltage dips, and sudden transmission line outages in the distribution network using the proposed method.
- Enabling the detection of fault location by OCRs in the distribution network in the presence of synchronous generator-based DG.
- Analyzing the impact of integrating output current control methods for synchronous generator-based DG using the proposed approach.

1.1 Motivation

Along with the benefits that connecting DG resources brings to the system, these resources may also have potential impacts on the operation, protection, and control of electrical transmission grids. The installation of these generators will result in a redistribution of load and, in some cases, may cause increased fault currents and overvoltage issues. A vital condition that enables the connection of distributed power sources to the grid is the establishment of proper coordination between the protection schemes of independently distributed generators and electric utility companies. In an efficient and coordinated protection system, faults are cleared in the shortest time possible, and the last portion of the system is severed due to a fault. Given the above points, conducting short-circuit

studies in the distribution system in the presence of DG resources, considering their effects on the grid, becomes increasingly necessary. The primary goal is to establish protection coordination in the distribution system with the presence of DG resources. Short-circuit studies serve as the foundation for protection coordination studies. In addition to conducting short-circuit studies, a transient stability analysis is also very important. The aim of performing transient stability studies in grid connection design studies is to calculate the CCT of a fault. This time is then utilized to coordinate the related protective relays. With the attachment of DG resources to the distribution system, due to the current injection from these resources during a fault, the protection system's performance may be disrupted. Inverter-based DG typically includes a current limiter, constraining the fault current injection to around 1 to 4 Pu, whereas DG based on synchronous or induction generators can inject fault currents ranging from 5 to 10 Pu [13]. This indicates more critical conditions for the protection system in the existence of synchronous generator-based DG. On the other hand, synchronous generator-based DG, with low inertia, can cause not only protection coordination issues but also transient stability disturbances during faults, jeopardizing the generators' safety due to mechanical hazards. Therefore, when connecting synchronous generator-based DG to the distribution network, the limitations in terms of stability and protection must be simultaneously considered in the protection designs. Challenges and solutions in grid integration are shown in Figure 1.

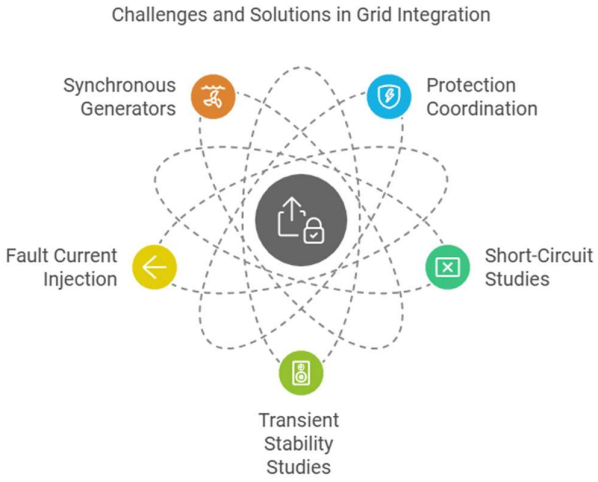

Figure 1. Barriers and Strategic Approaches in Grid Integration.

2. Case study of a network

The structure examined in this work to confirm the functionality of the proposed method is the IEEE 33 bus system. The test network is a radial configuration with a nominal power of 50 MVA and a nominal voltage level of 12.66 kV. The specifications of the IEEE 33 bus system under study and the DG sources connected to it are presented in the supplement. In this system, DG units relying on synchronous generators are utilized, with each source having a power level of one megawatt-hour. The locations of the DG sources are picked as buses 3, 9, 12, and 28 [9]. Considering the connection points of DG to the analyzed system, five scenarios are examined based on Table 1. As indicated in the Table, for every DG unit, two extra relays are implemented: A time-OCR is also implemented before the DG, and a time-OCR is also implemented after the DG. In this case, the time-OCR after the DG acts as the primary relay, while the time-OCR before the DG functions as a backup relay. Load flow emulation, short circuit examination, protection synchronization, and stability evaluations have been conducted using the ETAP application. The one-line protection schematic is exhibited in Figure 2.

Table 1. Scenarios were studied on the IEEE 33 bus system [28].

Scenario	Backup OCR	Primary OCR
1	OCR-1	OCR-2
2	OCR-1	OCR-3
3	OCR-4	OCR-5
4	OCR-6	OCR-7
5	OCR-8	OCR-9

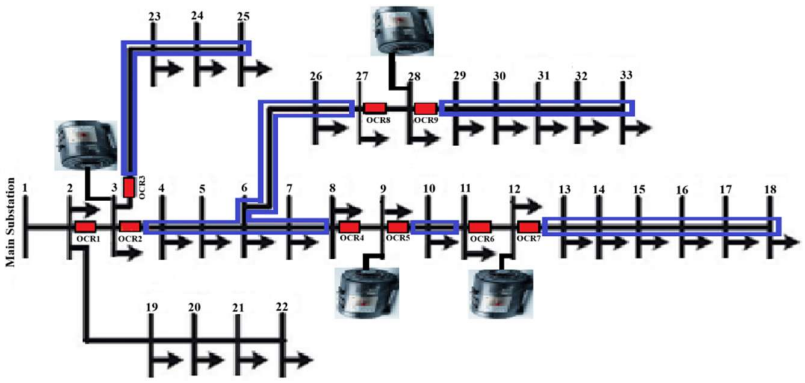

Figure 2. Protection-oriented one-line schematic of the analyzed network [28].

3. Proposed Technique

This article employs the ETAP application to develop a protective-stability algorithm, as shown in Figure 3, through a novel systematic method. First, protection research in the deficiency of DG units includes load flow examination to compute rated currents, short circuit examination to estimate fault currents, and relay coordination to confirm the CTI among primary and backup OCRs. Second, transient stability studies with joined DG units directly determine the CCT_{min} For each DG. Finally, the simultaneous confirmation of CTI and CCT is assessed, tackling two scenarios: when both CTI and CCT are accomplished, no adjustments are needed; however, if CTI is accomplished but CCT is not, the primary relay's TDS is reduced using specific equations to adjust the relay's inverse-time curve downward, ensuring both circumstances are fulfilled. K is a constant factor for coordinating overcurrent protection devices, which is set to 1.50 in this research, and the minimum TDS is 0.010 [28].

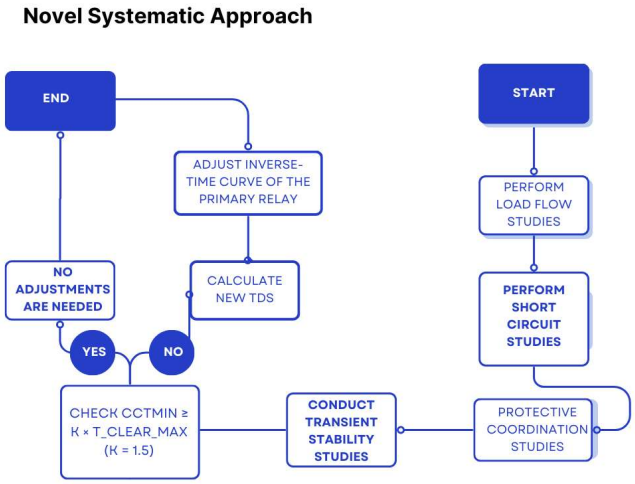

Figure 3. Proposed methodology.

3.1 OCR Coordination

OCRs are deemed one of the simplest and most effective approaches for power grid security. They are often utilized as the core protective equipment for radial configurations [11]. An OCR has two primary variables: the TMS and the PS. The relay's operating time is influenced by the TMS, the PS, and the current identified by the relay. The protective relay's nominal current is. The relay's operating time T_{op} is calculated using Equation (1) [29-32]. α, β, and γ are multipliers utilized to demonstrate a mathematical expression of the minimum inverse-time OCR

characteristic. These multipliers are established based on the overcurrent curve type following the IEC 60255 standard, as shown in Table 2 [33]. It is worth indicating that the typical inverse curve has been applied in this study.

$$T_{op} = \frac{\alpha \times TMS}{\left(\frac{I_f}{PS}\right)^{\beta} - \gamma} \tag{1}$$

$$PS = KI_n \tag{2}$$

$$PS_{imin} \leq PS_i \leq PS_{imax} \tag{3}$$

$$TMS_{imin} \leq TMS_i \leq TMS_{imax} \tag{4}$$

Table 2. IEC Standard Curve [33].

Parameters	Very reversal	Reversal normal	Short reversal	Extremely reversal	Long reversal
Alpha (α)	0.05	0.14	13.5	80	120
Beta (β)	0.4	0.02	1	2	1
Gamma (γ)	1	1	1	1	1

Each relay includes TMS and PS adjustments. The PS restriction is picked according to the highest feeder load current, the least fault current detected through the relay on the supply line, and the available relay adjustments. The TMS constraints are founded on the current attributes of the existing relay. These can be mathematically stated in the form of Equations (3) and (4). Each relay has a unique minimum operation time based on its manufacturing technique. Similarly, a relay should also have the longest operating time. This can be mathematically stated in the form of Equation (5).

$$t_{imin} \leq t_i \leq t_{imax} \tag{5}$$

In (5), t_{imin} is the minimum operating time of the relay for a fault at every spot on the downstream side of the relay, and t_{imax} it is the maximum operating time of the relay for a fault at every spot within the relay's region. A fault occurring within the relay's region can be detected simultaneously by both the primary relay and the backup relay. To prevent malfunction, the backup relay must confirm activation only if the primary relay is not functioning. According to Figure 4, if R_j as the primary relay for a fault at the location k and R_i If the backup relay is for the identical fault, the coordination limitation can be expressed mathematically as Equation (6).

$$T_{j,k} - T_{i,k} \leq \Delta t \tag{6}$$

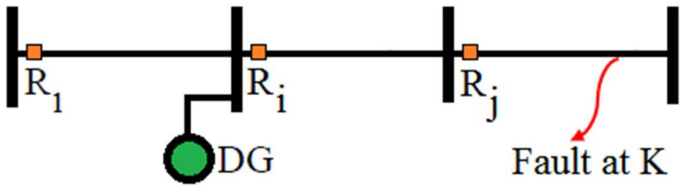

Figure 4. A typical power system includes DG sources with overcurrent protection.

In (6), $T_{i,k}$ is the operating time of the backup relay R_i for a fault in the protection area k, and $T_{j,k}$ is the operating time of the primary relay R_j for the same fault in the protection area k, Δt As the CTI [34]. According to Figure 5, the minimum CTI between two relays should not be less than 0.35 s [5]. As shown in the Fig, to confirm proper Protective harmonization between the two OCRs. R_i and R_j relay R_j St, function in the shortest possible time for a fault within its protection area. If the fault heightens, relay R_i to function at least 0.35 s after the function of the relay R_j.

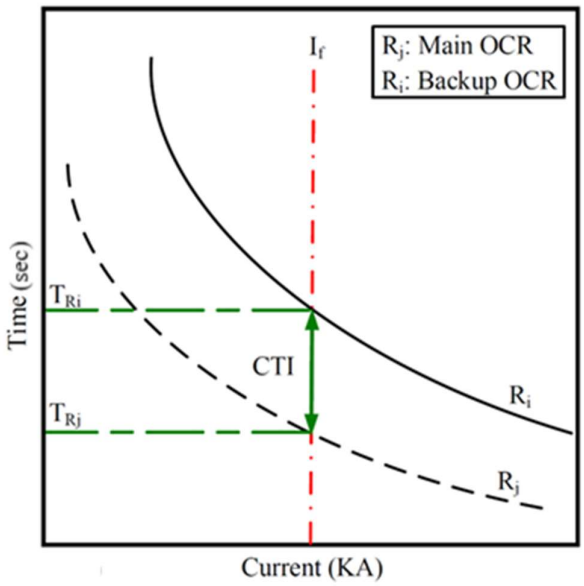

Figure 5. Establishing the CTI constraint between OCRs.

3.2 Synchronous Generator Stability

Transient stability in power grids is initiated by situations like short circuits, sudden line outages, or sudden excitation voltage drops in synchronous generators. The key indicator of stability or instability is the motion energy of the turbine units in the network. To assess the degree of stability of the network and generators against a specific disturbance, the maximum fault tolerance time can be applied. This is the critical fault CCT, which represents the maximum duration for clearing the fault while maintaining generator stability. A higher CCT indicates greater generator stability. The critical fault CCT (maximum fault tolerance time) of DG should be higher than the operating time of existing protective devices in the network. On the other hand, the minimum critical fault tolerance time for DG should be at least. k is the maximum relay operating time. k is the protection margin adjustable based on the type of DG, the network structure, the connection site, the DG penetration, and other factors? Therefore, for a given DG connection plan, the shortest critical fault tolerance time can be examined against the protection relay operating time using Equation (7) [28].

$$\mathrm{CCT}_{Min} \geq K \times T_{Clear-Max} \tag{7}$$

In (7), $T_{Clear-Max}$ is the maximum relay operating time. If the condition of Equation (7) is satisfied," the dynamic transient stability requirement for the DG integration scheme is satisfied. It is important to point out that in this case, the CCT value must fit within the following scope:

$$K \times T_{Clear-Max-\ j} \leq \mathrm{CCT}_{Min} < T_{Clear-R_i} \tag{8}$$

In (8), $T_{Clear-Ma\ \ j}$ is the maximum operating time of the primary relay, and $T_{Clear\ \ i}$ is the operating time of the backup relay? However, if the conditions specified in Equations (7) and (8) are not met, one of the following proposed methods must be executed. It is worth mentioning that the first method has been executed in this research work. The relay operating times should be re-adjusted so that the above conditions are satisfied. For this purpose, the new operating time of the primary OCR should be computed using Equation (9).

$$T_{R_j-new} = \frac{\alpha \times TMS_{new}}{\left(\frac{I_f}{PS}\right)^{\beta} - \gamma} \tag{9}$$

In (9), TMS_{new} As calculated/obtained from Equation (10) by combining Equation (1) and Equation (7). If the circumstance specified in Equation (7) is still not established after modifying the TDS value, the primary relay's inverse time characteristic curve, as shown in Figure 6, should be changed to a constant time type. This modification confirms that the relay functions in the shortest possible time for a fault within its protection area while also meeting the condition specified in Equation (7).

$$TMS_{new} = \frac{\frac{CCT_{Min}}{K} \times \left[\left(\frac{I_f}{PS}\right)^{\beta} - \gamma\right]}{\alpha} \tag{10}$$

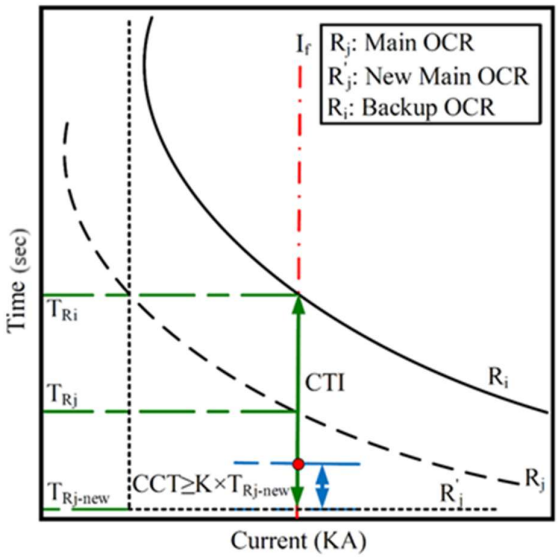

Figure 6. Modify the primary relay curve.

As shown in Figure 6, Equation (10) is also obtained by combining Equation (1) and Equation (7). This equation causes the time characteristic curve of the primary OCR. T_{Ri} to shift downward, and the CTI between the time characteristic curves of the primary OCR R_j and the backup OCR R_i Increases. According to Equation (10), the new time characteristic curve of the primary OCR T_{Rj-new} it is also generated. If transient stability cannot be obtained for the DG connection plan through the modifications in steps (1) and (2), and if connecting the DG to the network is crucial, the system must be equipped with an out-of-synchronism protection relay. This relay confirms that in the event of instability and loss of synchronism due to unknown conditions or disturbances, the relay will avoid major damage to the DG. To simultaneously increase the safeguarding and stability of the DG and the network, it is suggested that all DG units be equipped with out-of-synchronism protection devices.

4. Results & Discussion

Investigating the scenarios discussed in this research, as detailed with the standard settings of OCRs in Table 3, simulations of load flow, short circuit, protective coordination, and stability were conducted using the proposed algorithm within the ETAP software environment. In this research, a 3-phase fault scenario was also considered due to the resulting high fault current, which leads to voltage drops, network oscillations, and increased power losses. It is important to mention that the typical settings for the OCRs are presented in Table 4. After implementing the usual settings and subsequently evaluating the CTI amount, the TDS amount of the backup OCRs is modified (increased) if necessary to ensure that the CTI is maintained in the presence of DG. It is also noted that the maximum fault CCT from the system is thought to be 1s [5]. The results from the protective harmonization emulation to determine CT weak OCRs in the five defined scenarios are summarized in Table 4. As viewed in the Table, in the primary, secondary, tertiary, and fifth scenarios, to achieve a CTI of 0.35 s or greater, the newly computed TDS value for the secondary relays, based on Equation (6), has been elevated. However, in the fourth scenario, owing to the low fault

current, also with a decrease in the TDS amount to the lowest adjustable setting (0.010), the relays are unable to identify the fault. Therefore, to rectify this, in addition to adjusting the TDS amount for the secondary relays, the PS value of OCR-6 and OCR-7 relays has been diminished to 0.6 s. When the TMS is at its minimum value of 0.01 and cannot achieve the desired CTT of 0.35 seconds, a reduction in the PS is necessary. In industrial practice, this is typically set to 0.6 seconds. In the fifth scenario, to restrict the secondary relays' operating time to 1s, the TDS value for OCR-8 has been reduced.

Table 3. Standard settings of OCRs [35,36].

Current transformer conversion ratio	Curve type	TMS	PS
500/1	Normal reversal	0.10	1.20

Table 3 illustrates that the current transformer ratio is 500:1, the OCR characteristic is standard inverse, and the actual adjustments for the OCRs in the distribution system are TMS=0.10 and PS=1.20.

Table 4. Protective emulation conclusions for the scenarios studied on the IEEE 33 bus system [28].

Scenario	Backup OCR protection	Primary OCR protection	TMS (Primary OCR)	TMS (Backup OCR)	PS (Primary OCR)	PS (Backup OCR)	Fault bus	Operating time (s)		CTI (s)
								Primary OCR	Backup OCR	
1	OCR-1	OCR-2	0.10	0.220	1.20	1.20	Bus 8	0.227	0.645	0.418
							Bus 27	0.195	0.547	0.325
2	OCR-1	OCR-3	0.10	0.140	1.20	1.20	Bus 25	0.17	0.53	0.36
3	OCR4	OCR-5	0.10	0.140	1.20	1.20	Bus 11	0.314	0.677	0.363
4	OCR-6	OCR-7	0.10	0.140	0.60	0.60	Bus 18	0.296	0.653	0.357
5	OCR-8	OCR-9	0.070	0.070	1.20	1.20	Bus 33	0.514	0.92	0.406

Table 4 presents the protection results of the IEEE 33 bus network for scenario 1, where the primary and backup OCRs are (OCR1, OCR2), respectively. The TMS of the primary and backup OCRs are 0.10 and 0.220, respectively. The TMS of the primary OCRs is also 0.10, as per Table 3, and the TMS of the backup OCRs is obtained according to Equation (6). The PS of both the backup and primary OCRs is also 1.20, as specified in Table 3. When a fault occurs on Bus 8, the operating times of the primary and backup OCRs are 0.227 s and 0.645 s, respectively. The CTI between the primary and backup OCRs is 0.418 s. In the same scenario 1, with the same settings for the primary and backup OCRs, when a fault occurs on Bus 27, the operating times of the primary and backup OCRs are 0.195 s and 0.547 s, respectively. The CTI between the primary and backup OCRs is 0.325 s. In scenario 2, the primary and backup OCRs are (OCR1, OCR3), respectively. The TMS of the primary and backup OCRs are 0.10 and 0.140, respectively. The TMS of the primary OCRs is also 0.10, as per Table 3, and the TMS of the backup OCRs is obtained according to Equation (6). The PS of both the backup and primary OCRs is also 1.20, as specified in Table 3. When a fault occurs on Bus 25, the operating times of the primary and backup OCRs are 0.17 s and 0.53 s, respectively. The CTI between the primary and backup OCRs is 0.36 s. In scenario 3, the primary and backup OCRs are (OCR4, OCR5), respectively. The TMS of the primary and backup OCRs are 0.10 and 0.140, respectively. The PS of both the primary and backup OCRs is also 1.20. The TMS of the primary OCRs is also 0.10, as per Table 3, and the TMS of the backup OCRs is obtained according to Equation (6). The PS of both the backup and primary OCRs is also 1.20, as specified in Table 3. When a fault occurs on Bus 11, the operating times of the primary and backup OCRs are 0.314 s and 0.677 s, respectively. The CTI between the primary and backup OCRs is 0.363 s. In scenario 4, the primary and backup OCRs are (OCR6, OCR7), respectively. The TMS of the primary and backup OCRs are 0.10 and 0.140, respectively. The PS of both the primary and backup OCRs is also 0.60. The TMS of the primary OCRs is also 0.10, as per Table 3, and the TMS of the backup OCRs is obtained according to Equation (6). The PS of both

the backup and primary OCRs, when the TMS is at its minimum value of 0.010 and cannot achieve the desired CTI of 0.35 s (minimum TMS), needs to be reduced. In industrial practice, this is typically set to 0.60 s. When a fault occurs on Bus 18, the operating times of the primary and backup OCRs are 0.296 s and 0.653 s, respectively. The CTI between the primary and backup OCRs is 0.357 s. In scenario 5, the primary and backup OCRs are (OCR8, OCR9), respectively. The TMS of both the primary and backup OCRs is 0.070. The PS of both the primary and backup OCRs is also 1.20. The TMS of both the backup and primary OCRs is obtained as 0.07 according to Equation (10). The PS (PS) of both the backup and primary OCRs is also 1.20, as specified in Table 3. When a fault occurs on Bus 33, the operating times of the primary and backup OCRs are 0.514 s and 0.92 s, respectively. The CTI between the primary and backup OCRs is 0.406 s

To simultaneously apply the CTI and CCT limits, transient stability emulations of DGs (Distributed Generators) must be conducted. Subsequently, the condition in Equation (7) must be checked. If the condition is not fulfilled, the principal characteristic curve must be adjusted using Equations (9) and (10). In these cases, by lessening the TDS of the primary relay, not only is the CCT limit met, but the CTI limit is also enhanced. The outcomes of the transient stability emulations for DGs connected to the network are shown in Figures 7 to 10 and summarized in Table 5. Based on these figures, the CCT value for each DG is the time at which the generator speed or power angle achieves zero. As indicated in Table 5, the state in Equation (7) is only accomplished for scenario 3, and in scenarios 1, 2, 4, and 5, the state in Equation (7) is not achieved, and the TDS of the primary relay needs to be tuned.

Table 5. Results of generator transient stability modeling for the analyzed scenarios on the IEEE 33 bus system [28].

Scenario	Backup OCR protection	Primary OCR protection	Fault bus	Maximum operating time of the primary OCR	CCT (s)	CCT/K (s)	Equation (7) satisfaction
I	OCR-1	OCR-2	Bus 8	0.227	0.24	0.16	None
			Bus 27	0.195			None
II	OCR-1	OCR-3	Bus 25	0.17	0.24	0.16	None
III	OCR-4	OCR-5	Bus 11	0.314	0.51	0.34	Done
IV	OCR-6	OCR-7	Bus 18	0.296	0.38	0.253	None
V	OCR-8	OCR-9	Bus 33	0.514	0.22	0.147	None

Table 5 reveals the transient stability results of the IEEE 33 bus system in scenario one, which are the primary and backup OCRs (OCR-1, OCR-2), in turn. When a 3-phase fault happens in bus 8, the maximum execution time of the primary OCR is 0.227 s, which is greater than the condition of Equation (7), which is 0.16 s. In this case, the CCT of the synchronous generator fault is also 0.24 s. In scenario one, the primary and backup OCRs are OCR-1 and OCR-2. When a 3-phase fault happens in bus 27, the maximum execution time of the chief OCR is 0.195 s, which is greater than the condition of Equation (7), which is 0.16 s. In this case, the CCT of the synchronous generator fault is also 0.24 s. In scenario 2, with OCR-3 as the primary protection and OCR-1 as the backup, a 3-phase fault on bus 25 results in a maximum execution time of 0.17 s for the primary relay, exceeding the limit of 0.16 s specified by Equation (7). The CCT of the synchronous generator fault is 0.24 s. Scenario 3 implies that for a 3-phase fault on bus 11, where OCR-5 is the primary protection and OCR-4 is the backup, the maximum execution time of the primary relay is 0.314 s, which conforms with the limit of 0.34 s set by Equation (7). The CCT of the synchronous generator fault is 0.51 s. In scenario 4, with OCR-7 as the primary protection and OCR-6 as the backup, a 3-phase fault on bus 18 results in a maximum execution time of 0.296 s for the primary relay, exceeding the limit of 0.253 s specified by Equation (7). The CCT of the synchronous generator fault is 0.38 s. Scenario 5 shows that for a 3-phase fault on bus 33, where OCR-9 is the primary protection and OCR-8 is the backup, the maximum execution time of the primary relay is 0.514 s, which significantly exceeds the limit of 0.147 s set by Equation (7). The CCT of the synchronous generator fault is 0.51 s.

Figure 7 (a) shows that in scenarios 1 and 2, when a 3-phase fault current occurs at Buses 8, 27, and 25, the operating time of the primary OCR is 0.227 s, 0.195 s, and 0.17 s, respectively. In this case, the CCT of the synchronous generator 1 fault is 0.24 s with a synchronous generator 1 speed of 1800 RPM. The operating time of the primary OCR is greater than the condition specified in Equation (7), which is 0.16 s, leading to speed instability of synchronous generator 1. Figure 7 (b) shows that in scenarios 1 and 2, when a 3-phase fault current occurs at Buses 8, 27, and 5, the operating time of the primary OCR is 0.227 s, 0.195 s, and 0.17 s, respectively. In this case, the CCT of the synchronous generator 1 fault is 0.24 s with a synchronous generator 1 power angle of 84 degrees. The operating time of the primary OCR is greater than the condition specified in Equation (7), which is 0.16 s, leading to power angle instability of synchronous generator 1.

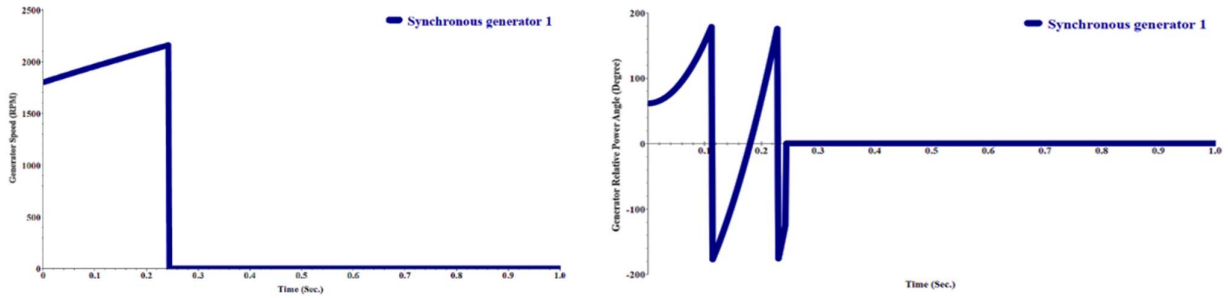

(a) (b)

Figure 7. Transient stability emulation of synchronous generator 1, (a) generator speed (RPM), (b) synchronous generator power angle (degrees).

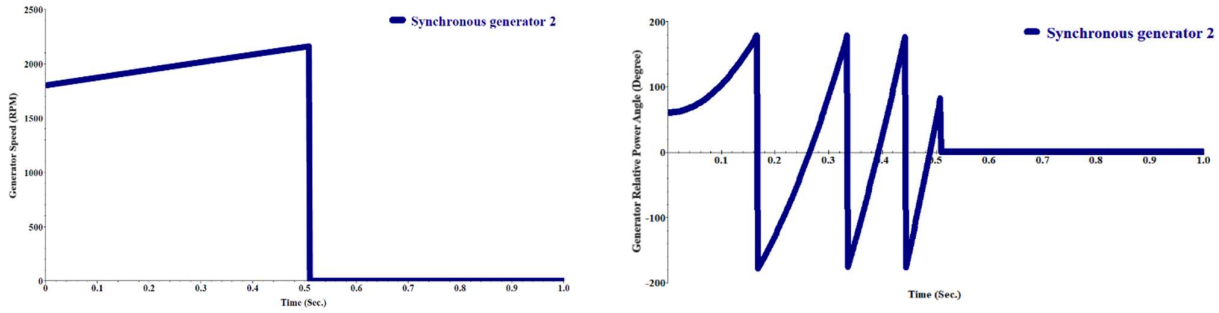

(a) (b)

Figure 8. Transient stability emulation of synchronous generator 2, (a) generator speed (RPM), (b) synchronous generator power angle (degrees).

Figure 8 (a) shows that in scenario 3, when a 3-phase fault current occurs at Bus 11, the operating time of the primary OCR is 0.314 s. In this case, the CCT of the synchronous generator 2 fault is 0.51 s with a synchronous generator speed of 1800 RPM. The operating time of the primary OCR is less than the condition specified in Equation (7), which is 0.34 s, leading to speed instability of synchronous generator 2. Figure 8 (b) shows that in scenario 1, when a 3-phase fault current occurs at Bus 11, the operating time of the primary OCR is 0.314 s. In this case, the CCT of the synchronous generator 2 fault is 0.51 s with a synchronous generator power angle of 84 degrees. The operating time of the primary OCR is less than the condition specified in Equation (7), which is 0.34 s, leading to power angle instability of synchronous generator 2.

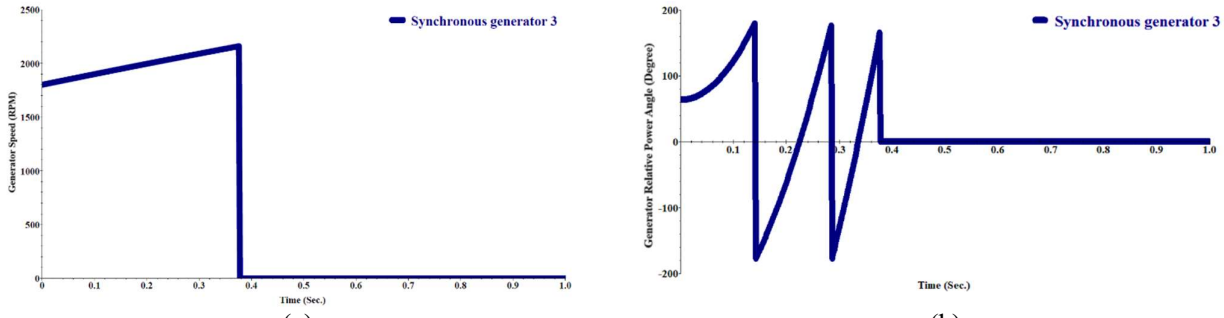

(a) (b)

Figure 9. Transient stability emulation of synchronous generator 3, (a) generator speed (RPM), (b) synchronous generator power angle (degrees).

Figure 9 (a) shows that in scenario 4, when a 3-phase fault current occurs at Bus 18, the operating time of the primary OCR is 0.296 s. In this case, the CCT of the synchronous generator 3 fault is 0.38 s with a synchronous generator speed of 1800 RPM. The operating time of the primary OCR is greater than the condition specified in Equation (7), which is 0.253 s, leading to speed instability of synchronous generator 3. Figure 9 (b) shows that in scenario 1, when a 3-phase fault current occurs at Bus 18, the operating time of the primary OCR is 0.296 s. In this case, the CCT of the synchronous generator 3 fault is 0.38 s with a synchronous generator power angle of 84 degrees. The operating time of the primary OCR is greater than the condition specified in Equation (7), which is 0.253 s, leading to power angle instability of synchronous generator 3.

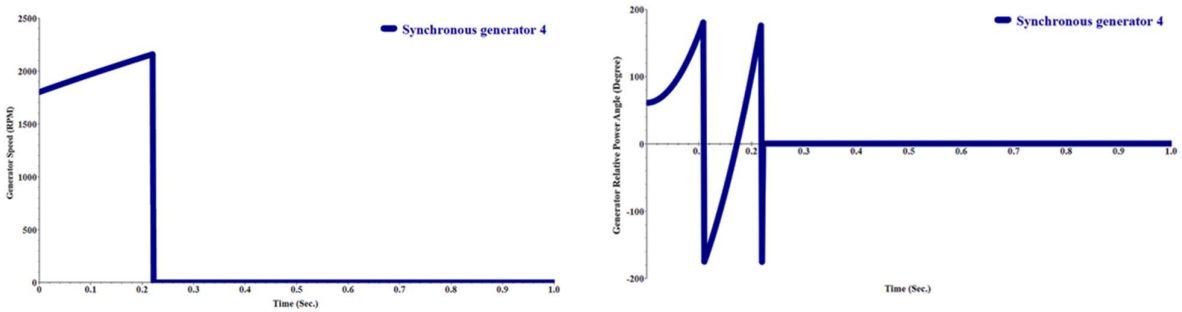

(a) (b)

Figure 10. Transient stability emulation of synchronous generator 4, (a) generator speed (RPM), (b) synchronous generator power angle (degrees)

Figure 10 (a) shows that in scenario 5, when a 3-phase fault current occurs at Bus 33, the operating time of the primary OCR is 0.514 s. In this case, the CCT of the synchronous generator 4 fault is 0.22 s with a synchronous generator speed of 1800 RPM. The operating time of the primary OCR is greater than the condition specified in Equation (7), which is 0.147 s, leading to speed instability of synchronous generator 4. Figure 10 (b) shows that in scenario 5, when a 3-phase fault current occurs at Bus 33, the operating time of the primary OCR is 0.514 s. In this case, the CCT of the synchronous generator 4 fault is 0.22 s with a synchronous generator power angle of 84 degrees. The operating time of the primary OCR is greater than the condition specified in Equation (7), which is 0.147 s, leading to power angle instability of synchronous generator 4.

The outcomes of the protective harmonization emulation with applying the CCT situation for scenarios one, two, four, and five, are shown in Figures 11 to 13. The results indicate that, in this issue, the TDS values of the primary relays decreased to simultaneously satisfy both the CTI and CCT limitations. It is worth mentioning that for a better understanding of the emulation outcomes, a recap of the results is given in Table 6. This depicts the approach of regulating the TDS of the primary relays to guarantee that, together, the CTI and CCT limitations are fulfilled in different scenarios.

Table 6. Results of protective emulation - stability of the studied scenarios on the IEEE 33 bus system [28].

Scenario	Backup OCR protection	Primary OCR protection	TMS (Primary OCR)	TMS (Backup OCR)	Fault bus	Operating time (s)		CTI (s)	CCT/K (s)
						Primary OCR	Backup OCR		
1	OCR-1	OCR-2	0.070	0.220	bus 8	0.159	0.547	0.486	0.16
					bus 27	0.136	0.645	0.411	0.16
2	OCR-1	OCR-3	0.090	0.140	bus 25	0.153	0.53	0.377	0.16
3	OCR-4	OCR-5	0.10	0.140	bus 11	0.314	0.677	0.363	0.34
4	OCR-6	OCR-7	0.080	0.140	bus 18	0.237	0.653	0.416	0.253
5	OCR-8	OCR-9	0.020	0.070	bus 33	0.147	0.92	0.773	0.147

Table 6 shows the protective-stability simulation results of the scenarios studied in the IEEE 33 bus test network. Scenario 1, where the primary and backup OCRs are OCR1, OCR2, respectively. The TMS of the primary and backup OCRs are 0.070 and 0.220, respectively. The TMS of the primary and backup OCRs, according to Equations

(10) and (6), respectively, are 0.070 and 0.220. When a fault occurs on Bus 8, the operating times of the primary and backup OCRs are 0.159 s and 0.547 s, respectively. The CTI between the primary and backup OCRs is 0.486 s. In this case, the CCT of the synchronous generator fault is 0.16 s. In the same scenario 1, with the same settings for the primary and backup OCRs, when a fault occurs on Bus 27, the operating times of the primary and backup OCRs are 0.136 s and 0.645 s, respectively. The CTI between the primary and backup OCRs is 0.411 s. In this case, the CCT of the synchronous generator fault is also 0.16 s. In scenario 2, the primary and backup OCRs are (OCR1, OCR3), respectively. The TMS of the primary and backup OCRs are 0.090 and 0.140, respectively. The TMS of the primary and backup OCRs, according to Equations (10) and (6), respectively, are 0.090 and 0.220. When a fault occurs on Bus 25, the operating times of the primary and backup OCRs are 0.153 s and 0.530 s, respectively. The CTI between the primary and backup OCRs is 0.377 s. In this case, the CCT of the synchronous generator fault is 0.16 s. In scenario 3, the primary and backup OCRs are (OCR4, OCR5), respectively. The TMS of the primary and backup OCRs are 0.10 and 0.140, respectively. The TMS of the primary and backup OCRs, according to Equations (6) and (6), respectively, are 0.10 and 0.140. When a fault occurs on Bus 11, the operating times of the primary and backup OCRs are 0.314 s and 0.677 s, respectively. The CTI between the primary and backup OCRs is 0.363 s. In this case, the CCT of the synchronous generator fault is 0.34 s. In scenario 4, the primary and backup OCRs are (OCR6, OCR7), respectively. The TMS of the primary and backup OCRs are 0.080 and 0.140, respectively. The TMS of the primary and backup OCRs, according to Equations (10) and (6), respectively, are 0.080 and 0.140. When a fault occurs on Bus 18, the operating times of the primary and backup OCRs are 0.237 s and 0.653 s, respectively. The CTI between the primary and backup OCRs is 0.416 s. In this case, the CCT of the synchronous generator fault is 0.253 s. In scenario 5, the primary and backup OCRs are (OCR8, OCR9), respectively. The TMS of the primary and backup OCRs are 0.020 and 0.070, respectively. The TMS of the primary and backup OCRs, according to Equations (10) and (6), respectively, are 0.020 and 0.070. When a fault occurs on Bus 33, the operating times of the primary and backup OCRs are 0.147 s and 0.92 s, respectively. The CTI between the primary and backup OCRs is 0.773 s. In this case, the CCT of the synchronous generator fault is 0.147 s.

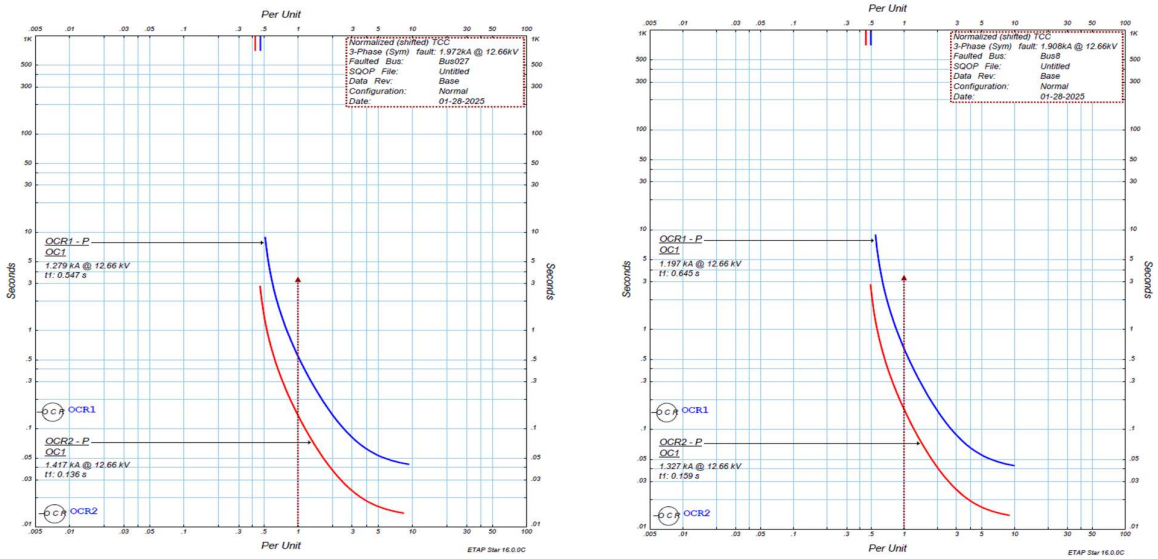

Figure 11. (a) Coordination between OCRs in scenario 1 for bus 27, (b) coordination between OCRs in scenario 1 for bus 8

Figure 11 (a) shows that in scenario 1, with a voltage level of 12.66 kV, when a 3-phase fault occurs on bus 27 with a fault current level of 1.279 kA, the operation time of the primary OCR (OCR2) is 0.136 s at a fault current of 1.417 kA, and the operation time of the backup OCR (OCR1) is 0.547 s at a fault current of 1.279 kA. In this case, the CTI between the characteristic curves of the primary and backup OCR (OCR2-OCR1) is 0.411 s. Figure 11 (b) shows that in scenario 1, with a voltage level of 12.66 kV, when a 3-phase fault occurs on bus 8 with a fault current level of 1.908 kA, the operation time of the primary OCR (OCR2) is 0.159 s at a fault current of 1.327 kA, and the operation time of the backup OCR (OCR1) is 0.645 s at a fault current of 1.197 kA. In this case, the CTI between the characteristic curves of the primary and backup OCR (OCR2-OCR1) is 0.486 s.

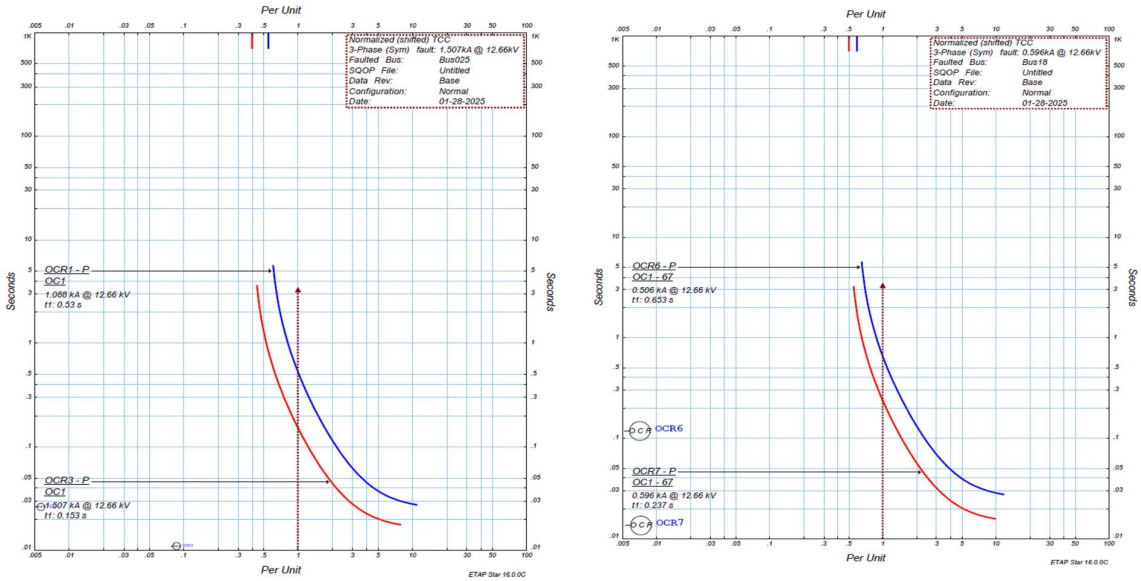

Figure 12. (a) Coordination between OCRs in scenario 2 for bus 25, (b) coordination between OCRs in scenario 4 for bus 18

Figure 12 (a) shows that in scenario 2, with a voltage level of 12.66 kV, when a 3-phase fault occurs on bus 25 with a fault current level of 1.507 kA, the operation time of the primary OCR (OCR3) is 0.153 s at a fault current of 1.507 kA, and the operation time of the backup OCR (OCR1) is 0.53 s at a fault current of 1.088 kA. In this case, the CTI between the characteristic curves of the primary and backup OCR (OCR3-OCR1) is 0.377 s. Figure 12 (b) shows that in scenario 4, with a voltage level of 12.66 kV, when a 3-phase fault occurs on bus 18 with a fault current level of 0.596 kA, the operation time of the primary OCR (OCR7) is 0.237 s at a fault current of 0.596 kA, and the operation time of the backup OCR (OCR6) is 0.653 s at a fault current of 0.506 kA. In this case, the CTI between the characteristic curves of the primary and backup OCR (OCR7-OCR6) is 0.416 s.

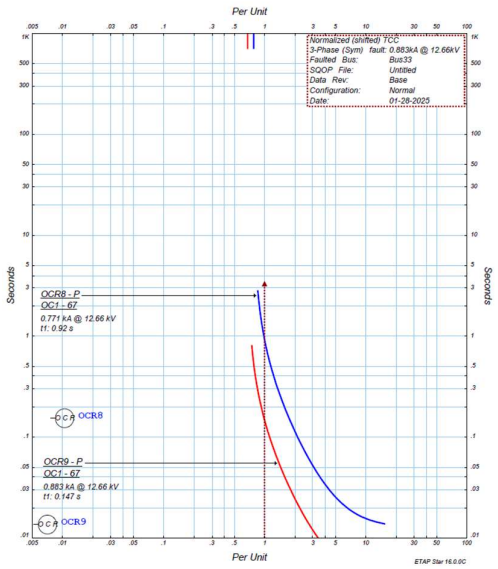

Figure 13. Coordination between OCRs in scenario 5 for Bus 33.

Figure 13 shows that in scenario 5, with a voltage level of 12.66 kV, when a 3-phase fault occurs on bus 33 with a fault current level of 0.883 kA, the operation time of the primary OCR (OCR9) is 0.147 s at a fault current of 0.833

kA, and the operation time of the backup OCR (OCR8) is 0.92 s at a fault current of 0.771 kA. In this case, the CTI between the characteristic curves of the primary and backup OCR (OCR9-OCR8) is 0.773 s.

Table 7. Comparison of the previous research.

Reference	Research area	Key consideration	Limitation	Main finding	Summary
[10]	Power system stability	DG, Relay coordination, Stability	This study considers directional OCRs in the presence of DG sources	Using a protective algorithm to optimize directional OCRs in the presence of DG sources.	This research presents a protective algorithm that coordinates and optimizes directional OCRs.
[16]	Distribution system protection	Protection, Transient stability, and Relay coordination	This study focuses on directional OCRs	Protective harmonization between directional OCRs and transient stability against faults in the presence of distributed resources	This study presents a protective harmonization method between directional relays, which improves the transient stability of distributed resources against load variations and faults.
[17]	DG resources	Reliability, Technical impacts	This study is solely focused on the integration of DG resources in the DIgSILENT Power Factory software.	Integration of DG resources and power quality in DIgSILENT Power Factory software	This article discusses the integration of various types of DG sources and enhances the power quality of the grid against harmonics.
[21]	Distribution network	Directional OCRs, Protection, DG	In this paper, a hybrid optimization algorithm, GA-NLP, is used for fault location analysis.	Utilizing the hybrid optimization algorithm GA-NLP also enhances relay sensitivity for minimum fault currents and improves relay operating speed for maximum fault currents.	This research also analyzes fault location using the hybrid optimization algorithm GA-NLP.
[23]	Protection of distribution systems	Distribution Network, OCR Coordination, Protection	This study also focuses solely on the reduced coordination times between OCRs using PSO, GA, TLBO, and SFLA algorithms	This approach utilizes the aforementioned four algorithms to determine the reduced coordination times in OCRs on an IEEE 33 bus distribution system.	This research also determines the reduced operating times of OCRs using the aforementioned algorithms and improves the performance time of OCRs.
[24]	Protection of distribution networks	Overcurrent Protection, DG	This study also utilized PSO and GA to reduce the operating time of OCRs.	An optimal coordination scheme for fault location in an IEEE 9-bus network using PSO and GA algorithms.	This paper also enhances the coordination between OCRs for fault detection using PSO and GA algorithms.
[26]	Protection of grid-connected MGs	Protection, DG	This study focuses solely on unbalanced faults and high-resistance faults.	Application of the dynamic impedance angle method for detection of unbalanced and high-resistance faults using MATLAB on an IEEE 34-bus network	This research also addresses unbalanced faults using the dynamic impedance angle method.
[28]	Power System Protection	Transient Stability, Protection, DG	This study focuses on the time constraint between OCRs	Improving the stability of DG by adjusting the time constraints between OCRs.	This research presents a protective method to support DG sources against transient instability.

This study	Transient stability examination	Fault clearing time	The study does not cover other types of DGs.	The study demonstrated that adjusting the TDS of the primary OCR can satisfy both the CTI and CCT conditions, preventing instability in synchronous generator DGs under fault conditions.	This inquiry investigates the transient stability of a distribution network with synchronous generator DGs, emphasizing fault-clearing times and protection coordination to prevent instability, and proposes future research directions to enhance system stability and efficiency.
	This research presents an innovative systematic method for transient stability assessment, enhancing relay coordination time, achieving simultaneous compliance with CCT and CTI constraints, and performing straightforward calculations without reliance on external equipment. Furthermore, this research discusses scenarios involving 3-phase faults or the occurrence of sequential faults, which may arise in real-world networks.				

5. Conclusion

Despite its advantages, interconnecting synchronous generators to the distribution network presents certain difficulties, including the possibility of transitory 3-phase faults and the injection of fault currents. Both the distribution network and the synchronous generators themselves may become unstable as a result of these. Distribution network breakdowns can result in voltage decreases, higher power losses, network fluctuations, and a breakdown in protective relay synchronization. Nevertheless, this coordination is missing from cases 1, 2, 4, and 5. Coordination between primary and backup OCRs can be formed by implementing the suggested technique and modifying the TMS of the OCRs in each case. By increasing the CTI between the primary and backup OCRs' characteristic curves, this ensures that the primary OCR eliminates the fault more quickly in any situation. This meets the coordination requirement between the CCT and CTI and avoids synchronous generator instability in the distribution network. The findings of this protective technique suggest further studies. These include testing the protection method on different networks, looking into protective coordination with other DG types, and analyzing the coordination of additional protection mechanisms like relay-fuse combinations, relay-reclosers, recloser-fuses, and distinct DGs.

Appendix:

Synchronous generators (SGs)				*3 kV*	$r_{st} = 0.09\ pu$	$X_l = 0.14\ pu$	$X_d = X_q = 1.55\ pu$
1	2	3	4		$X_d^{'} = 0.25pu$	$X_q^{'} = 0.6\ pu$	$X_d^{''} = 0.2u$
1 MVA	1 MVA	1 MVA	1 MVA		$X_q^{''} = 0.6u$	*H=nominal MVA*	
Setup Transformers				*12.66/3kV*		$U_k = 6\%$	$\frac{x}{r} = 8.5$

Acronyms:

Abbreviation	Definition	Abbreviation	Definition
Distributed generation	DG	Microgrid	MG
Time Multiplier Setting	TMS	Genetic Algorithm	GA
Plug Setting	PS	Traveling Waves	TW
Critical Clearing Time	CCT	Discrete Wavelet Transform	DWT
Time Dial Setting	TDS	Particle Swarm Optimization	PSO
Coordination Time Interval	CTI	Teaching-Learning-Based Optimization	TLBO
Overcurrent Relay	OCR	Shuffled Frog Leaping Algorithm	SFLA
Combined Heat and Power	CHP	Adaptive Fuzzy Directional Bat Algorithm	AFDBA
International Electrotechnical Commission	IEC	Natural Language Processing	NLP
Institute of Electrical and Electronics Engineers	IEEE	Directional Overcurrent Relay	DOCR

Active Current Limiting Control	ACLC	Three-Phase	3-phase
Hunger Games Search	HGS	Per unit	Pu
Grey Wolf Optimization	GWO	Kilovolt-Ampere Reactive	kVAR
Cuckoo Search	CS	Kilovolt	kV
Vehicle-Two-Grid	V2G	Megavolt-Ampere	MVA
Modified Hunger Games Search	MHGS	Megawatt	MW
Multi-Agent System	MAS	Second	s
Inverse-Definite Minimum Time	IDMT	Primary relay	R_j
Constant factor	k	Backup relay	R_i
Operating time of the relay	T_{op}	Fault current	I_f
Constant coefficients for different types of overcurrent relays	α, β, γ	Nominal current	I_n
Value of the time multiplier setting for relay i	TMS_i	Minimum Time multiplier setting value of the relay R_i	$TMS_{i,min}$
The maximum time multiplier setting value of the relay R_i	$TMS_{i,max}$	Value of the plug setting for relay i	PS_i
Minimum plug setting for relay i	$PS_{i,min}$	Maximum plug setting for relay i	$PS_{i,max}$
Operating time of a relay	t_i	Minimum critical clearing time	CCT_{min}
Minimum operating time of the relay	t_{imin}	The maximum operating time of the relay	$T_{Clear-Max}$
Maximum operating time of the relay	t_{imax}	The maximum operating time of the primary relay	$T_{Clear-Max-R_j}$
Operating time of the backup relay $R_{i,}$ for the fault in zone k	$T_{i,k}$	The operating time of the backup relay	$T_{Clear-R_i}$
Operating time of the primary relay $R_{j,}$ for the fault in zone k	$T_{j,k}$	New operating time of the primary overcurrent relay	T_{Rj-new}
Δt is the coordination time interval	Δt	New time multiplier setting.	TMS_{new}

DECLARATIONS

Conflict of Interest: The authors declare that there is no conflict of interest.
Funding: This research received no external funding.
Availability of data and materials: No data is available in this article.
Publisher's note: The Journal and Publisher remain neutral about jurisdictional claims in published maps and institutional affiliations.
Acknowledgments
The authors would like to formally acknowledge *Mr. Alireza Zabihi* for his exceptional guidance.

REFERENCES

[1]. Zabihi A, Parhamfar M. Decentralized energy solutions: The impact of smart grid-enabled EV charging stations. *Heliyon*. 2025;19:e41815. https://doi.org/10.1016/j.heliyon.2025.e41815
[2]. Zhang X, Karady GG, Ariaratnam ST. Optimal allocation of CHP-based distributed generation on urban energy distribution networks. *IEEE Trans Sustain Energy*. 2014;5(1):246–53. https://doi.org/10.1109/TSTE.2013.2278693
[3]. Chatterjee P, Khorsand M, Hedman KW. Enhanced assessment of power system behavior during multiple contingencies. In: *2018 North American Power Symposium (NAPS)*; 2018 Sep 9–11; Fargo, ND, USA. https://doi.org/10.1109/NAPS.2018.8600687
[4]. Bhusal N, Abdelmalak M, Kamruzzaman M, Benidris M. Power system resilience: current practices, challenges, and future directions. *IEEE Access*. 2020;8:18064–86. https://doi.org/10.1109/ACCESS.2020.2968586
[5]. Fani B, Bisheh H, Karami-Horestani A. An offline penetration-free protection scheme for PV-dominated distribution systems. *Electr Power Syst Res*. 2018;157:1 9. https://doi.org/10.1016/j.epsr.2017.11.020
[6]. Hajimohammadi F, Fani B, Sadeghkhani I. Fuse saving scheme in highly photovoltaic-integrated distribution networks. *Int Trans Electr Energy Syst*. 2020;30:e12148. https://doi.org/10.1002/2050-7038.12148
[7]. Ren C, Liu RP, Yin W, Long Q, Hou Y. Resilience assessment of mobile emergency generator-assisted distribution networks: A stochastic geometry approach. *J Econ Technol*. 2023;1:48 74. https://doi.org/10.1016/j.ject.2023.10.002
[8]. Razzaghi R, Davarpanah M, Sanaye-Pasand M. Novel Protective Scheme to Protect Small-Scale Synchronous Generators Against Transient Instability. *IEEE Trans Ind Electron*. 2013;60(4):1659–67. https://doi.org/10.1109/TIE.2012.2186773
[9]. Aghdam TS, Karegar HK, Zeineldin HH. Transient Stability Constrained Protection Coordination for Distribution Systems With DG. *IEEE Trans Smart Grid*. 2018;9(6):5733–41. https://doi.org/10.1109/TSG.2017.2695378

[10]. Aghdam TS, Karegar HK, Zeineldin HH. Optimal coordination of double-inverse overcurrent relays for stable operation of DGs. *IEEE Trans Ind Inform*. 2019;15(1):183–92. https://doi.org/10.1109/TII.2018.2808264
[11]. Nayanatara C, Shanmugapriya P, Baskaran J, Sharmila P. Overcurrent and Earthfault Relay Coordination for Microgrid with Numerical Relay Features. *Int J Innovative Technol Explor Eng*. 2020;9(3). https://doi.org/10.35940/ijitee.C8456.019320
[12]. Baeckeland N, Herteleer B, Kleemann M. Modelling fault behaviour of power electronic converters. *Int J Electr Power Energy Syst*. 2020;123:106230. https://doi.org/10.1016/j.ijepes.2020.106230
[13]. Qian Z, Yuan Y, Li J, Dong H, Qin T, Huang X. A Two-Stage Protection Scheme Based on Control and Protection Coordination for AC/DC Hybrid Distribution Network. *IEEE Access*. 2024;12:132533–42. https://doi.org/10.1109/ACCESS.2024.3457836
[14]. Abdelfattah W, Nagy A, Salama MM, Lotfy ME, Abdelhadi H. Artificial intelligence-based optimal coordination of directional overcurrent relay in distribution systems considering vehicle-to-grid technology. *Ain Shams Eng J*. 2024;15(2):102372. https://doi.org/10.1016/j.asej.2023.102372
[15]. Merabet O, Kheldoun A, Bouchahdane M, Eltom A, Kheldoun A. An adaptive protection coordination for microgrids utilizing an improved optimization technique for user-defined DOCRs characteristics with different groups of settings, considering N-1 contingency. *Expert Syst Appl*. 2024;248:123449. https://doi.org/10.1016/j.eswa.2024.123449
[16]. Sheta AN, Sedhom BE, Pal A, El Moursi MS, Eladl AA. Stability-Constrained Settings of Directional Overcurrent Relays With Shifted User-Defined Characteristics for Distribution Networks With DERs. *IEEE Trans Power Deliv*. 2024;39(4):2401–13. https://doi.org/10.1109/TPWRD.2024.3403921
[17]. Eidiani M, Zeynal H, Zakaria Z. Comprehensive Study on The Renewable Energy Integration Using DIgSILENT. In: *2023 IEEE 3rd Int. Conf. Power Eng. Appl. (ICPEA)*; 2023 Mar 6–7; Putrajaya, Malaysia. https://doi.org/10.1109/ICPEA56918.2023.10093153
[18]. Eladl AA, Sheta AN, Saeed MA, Bureš V, Sedhom BE. Assessing the impact of distributed energy resources on overcurrent protection in microgrids for enhanced effectiveness. *Results Eng*. 2025;25:104461. https://doi.org/10.1016/j.rineng.2025.104461
[19]. Saber A, Abdelemam AM, Zeineldin HH, El-Saadany EF. Time-domain protection scheme for inverter-dominated islanded microgrid using low-bandwidth communication channels. *Int J Electr Power Energy Syst*. 2025;165:110485. https://doi.org/10.1016/j.ijepes.2025.110485
[20]. Eladl AA, Sheta AN, Elgamal M, Vasquez JC, Sedhom BE. Optimal directional overcurrent relay settings for stable microgrids with synchronous and inverter-based resources. *Int J Electr Power Energy Syst*. 2025;167:110639. https://doi.org/10.1016/j.ijepes.2025.110639
[21]. Tripathi M, Mallik SK. An adaptive protection coordination strategy utilizing user-defined characteristics of DOCRs in a microgrid. Electr Power Syst Res. 2023;214:108900. https://doi.org/10.1016/j.epsr.2022.108900
[22]. Aboelezz AM, El-Afifi MI, Sedhom BE, Eladl AA, Sanjeevikumar P, Sheta AN. Advanced centralized protection system for AC microgrids using TW-DWT techniques. Energy Convers Manag X. 2025;25:100852. https://doi.org/10.1016/j.ecmx.2024.100852
[23]. Saldarriaga-Zuluaga SD, López-Lezama JM, Muñoz-Galeano N. Adaptive protection coordination scheme in microgrids using directional over-current relays with non-standard characteristics. Heliyon. 2021;7(4):e06665. https://doi.org/10.1016/j.heliyon.2021.e06665
[24]. Alasali F, El-Naily N, Zarour E, Saad SM. Highly sensitive and fast microgrid protection using optimal coordination scheme and nonstandard tripping characteristics. Int J Electr Power Energy Syst. 2021;128:106756. https://doi.org/10.1016/j.ijepes.2020.106756
[25]. Díaz Caicedo AM, Franco Mejia É, Gómez Luna E. Revolutionizing protection dynamics in microgrids: Local validation environment and a novel global management control through multi-agent systems. Comput Electr Eng. 2024;120:109748. https://doi.org/10.1016/j.compeleceng.2024.109748
[26]. Pradhan R, Jena P. An innovative fault direction estimation technique for AC microgrid. Electr Power Syst Res. 2023;215:108997. https://doi.org/10.1016/j.epsr.2022.108997
[27]. Sampaio FC, Tofoli FL, Melo LS, Barroso GC, Sampaio RF, Leão RPS. Adaptive fuzzy directional bat algorithm for the optimal coordination of protection systems based on directional overcurrent relays. Electr Power Syst Res. 2022;211:108619. https://doi.org/10.1016/j.epsr.2022.108619
[28]. Taheri M, Shahgholian G, Fani B, Mosavi A, Fathollahi A. A Protection Methodology for Supporting Distributed Generations concerning Transient Instability. In: 2023 IEEE 17th Int. Symp. Appl. Comput. Intell. Informat. (SACI); 2023 May 23–26; Timisoara, Romania. p. 1–6. https://doi.org/10.1109/SACI58269.2023.10158594
[29]. Niranjan P, Choudhary NK, Singh N, Singh RK. Optimal Coordination of Dual-Setting Directional Over Current Relay in Microgrid Considering Multi-Parametric Characteristics. J Oper Autom Power Eng. 2025;13(2):174–83. https://doi.org/10.22098/JOAPE.2023.12725.1965
[30]. Alasali F, El-Naily N, Mustafa HY, Loukil H, Saad SM, Saidi AS, et al. Innovative protection schemes through hardware-in-the-loop dynamic testing. Comput Electr Eng. 2024;119:109559. https://doi.org/10.1016/j.compeleceng.2024.109559
[31]. Kuriakose A, Balamurugan S. Optimum Overcurrent Relay Coordination in Radial System using Particle Swarm Optimization. In: 2023 IEEE 7th Conf. Inf. Commun. Technol. (CICT); 2023 Dec 15–17; Jabalpur, India. p. 1–6. https://doi.org/10.1109/CICT59886.2023.10455379

[32]. Elsadd M, Abd El-Ghany HA, Zaky M, Abdelaziz AY, Ahmed E. Optimum Coordination Approach for Directional Overcurrent Relays in Interconnected Power Systems Considering Uncertainty in Photovoltaic Generation. SSRN. 2024. https://doi.org/10.2139/ssrn.4703667

[33]. Beder H, Mohandes B, El Moursi MS, Badran EA, El Saadawi MM. A New Communication-Free Dual Setting Protection Coordination of Microgrid. IEEE Trans Power Deliv. 2021;36(4):2446–58. https://doi.org/10.1109/TPWRD.2020.3041753

[34]. Kalage AA, Ghawghawe ND. Optimum Coordination of Directional Overcurrent Relays Using Modified Adaptive Teaching Learning Based Optimization Algorithm. Intell Ind Syst. 2016;2:55 71. https://doi.org/10.1007/s40903-016-0038-9

[35]. Rojnić M, Prenc R, Topić D, Strnad I. A new methodology for optimization of overcurrent protection relays in active distribution networks regarding thermal stress curves. Int J Electr Power Energy Syst. 2023;152:109216. https://doi.org/10.1016/j.ijepes.2023.109216

[36]. K A, V C. Design of adaptive protection coordination scheme using SVM for an AC microgrid. Energy Rep. 2024;11:4688–712. https://doi.org/10.1016/j.egyr.2024.04.021

[37]. Shojaeian S, Parhamfar M. An experience in the design, implementation, and testing of concrete encased grounding electrode for a residential building. J Res Eng Appl Sci. 2023;8(1):476–82.

[38]. Parhamfar M, Shojaeian S, Bandegani Z. Feasibility Study and Design of Smart Low-Energy Building Electrical Installations (Case Study: Isfahan University, Virtual Faculty Building). Energy. 2023;6(3). http://dx.doi.org/10.25729/esr.2023.03.0006

[39]. Parhamfar M, Zabihi A. Comprehensive Design of a 100-Kilowatt Solar Power Plant with Bifacial Technology in PVsyst for Arak, Iran. Solar Energy Adv. 2025:100092. https://doi.org/10.1016/j.seja.2025.100092

[40]. Parhamfar, M. Towards Green Airports: Factors Influencing Greenhouse Gas Emissions and Sustainability through Renewable Energy. Next Res. 2024:100060. https://doi.org/10.1016/j.nexres.2024.100060

[41]. Taheri, S. H., Tayebati, P., & Parhamfar, M. (2025). Sustainable Strategies for Energy Management in Buildings and Electric Vehicle Charging. *Journal of Modern Technology*, *2*(01), 220-234. https://doi.org/10.71426/jmt.v2.i1.pp220-

[42]. Soma AK. Building Aether Sensor Network using LoRaWAN Network. In 2025 International Conference on Emerging Systems and Intelligent Computing (ESIC) 2025 Feb 8 (pp. 807-814). IEEE. 10.1109/ESIC64052.2025.10962750

[43]. Soma AK. Weighted Graph Clustering with PaCCo. In2025 International Conference on Emerging Systems and Intelligent Computing (ESIC) 2025 Feb 8 (pp. 815-818). IEEE. doi: 10.1109/ESIC64052.2025.10962723.

[44]. Parhamfar, M. (2025). A Novel Software Introduction for Enhanced Low-Voltage Electrical Installation Design in Buildings: VOLTA. *Journal of Modern Technology*, *2*(01), 246-253. https://doi.org/10.71426/jmt.v2.i1.pp246-253